



1991010781

A COMPARISON OF CFD PREDICTIONS AND EXPERIMENTAL RESULTS FOR A MACH 5 INLET

Lois J. Weir
NASA Lewis Research Center
Cleveland, Ohio

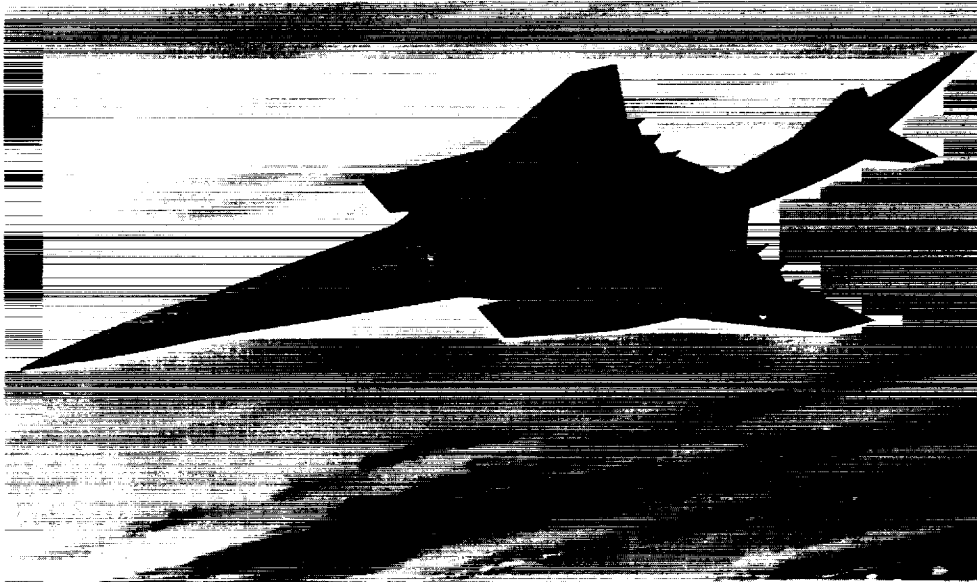
and

D.R. Reddy
Sverdrup Technology, Inc.
Lewis Research Center Group
Brook Park, Ohio

Flow through a high-speed, nominally two-dimensional inlet is characterized by highly complex, three-dimensional flow phenomena including strong secondary flows and shock/boundary layer interactions. In this paper, experimental and analytical data are presented for a Mach 5 mixed-compression inlet that exhibits such three-dimensional flow characteristics. The two-dimensional inlet model, designed to provide performance information in the Mach 3 to 5 speed range for an "over-under" turbojet plus ramjet propulsion system, was also instrumented to provide computational fluid dynamics (CFD) code calibration and validation data, and, in particular, to provide some detailed data in regions where three-dimensional phenomena dominate the local flow field. Calculations of the inlet flow field presented include three-dimensional parabolized and full Navier-Stokes code analyses, with and without bleed. CFD analyses predicted flow migration up the inlet sidewalls due to glancing shock/boundary layer interactions, which, in turn, developed patterns of vortical flow in the inlet. This vortical flow was at least partially captured by the cowl, which set up large regions of low-energy flow in the corners underneath the cowl. As the vortical flow stream passed through the strong cowl shock, its vorticity appeared to be somewhat dissipated and the low-energy flow was compressed against the cowl.

Comparisons between analytical predictions and experimental results are presented for rakes located in regions of vortical flow, separation, or both in the corners between the cowl and the sidewalls. Both experimental and analytical results indicated that porous bleed upstream on the inlet sidewalls and in the corners of the cowl had little effect on the vortical flow entering the inlet; however, bleed removed farther downstream near the shoulder (after the rotational flow had passed through the cowl shock) appeared to remove the low-energy flow on the cowl and sidewalls rather effectively.

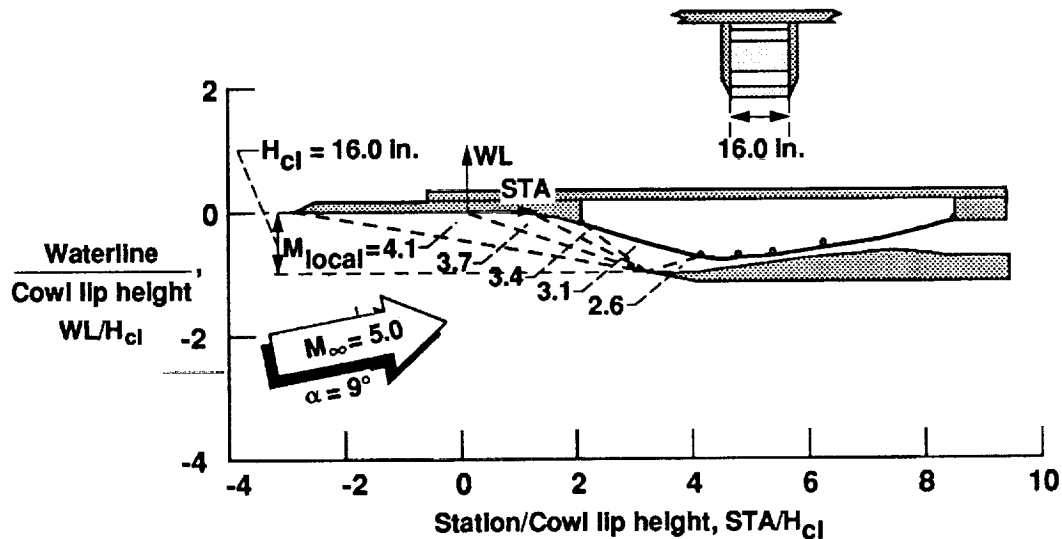
Artist's Concept of Mach 5 Cruise Aircraft



CD-91-53926

A joint research program between NASA Langley, NASA Lewis, and Lockheed (with Pratt & Whitney as a subcontractor) was begun in 1980 to investigate the critical flight technology issues in the Mach 3 to 5 speed range. The specific purpose of this study was to develop a concept for a Mach 5 penetrator aircraft, which is shown here. An over-under turbojet/ramjet propulsion system was chosen for this aircraft on the basis of size and weight considerations and ability to integrate with the airframe. Four of these propulsion systems were to be employed by the aircraft, two under each wing; and two-dimensional, dual-flow inlets were specified. A subsequent study resulted in the design of the lower (ramjet) portion of the inlet, which provides airflow in the Mach 3 to 5 speed range (ref. 1). A mixed-compression inlet model was designed for testing in the NASA Lewis 10- by 10-Foot Supersonic Wind Tunnel.

Inlet Design Contours



CD-91-53927

The inlet design contours are presented here. The inlet was designed such that at Mach 5 cruise conditions, the incoming airflow was at an angle of attack α of 9° relative to the first ramp. This ramp decelerated the flow to Mach 4.1. Two fixed ramps each provided 5° more compression. The last ramp, which was variable for off-design operation, compressed the flow an extra 5° at Mach 5. The cowl lip provided 10° of compressive turning, and the cowl shock was canceled on the inlet shoulder at design conditions. Internal isentropic compression of 11° further decelerated the flow into the inlet throat. The variable ramp surfaces were hinged at the locations shown, and a slip joint was located near the last hinge to compensate for changes in length.

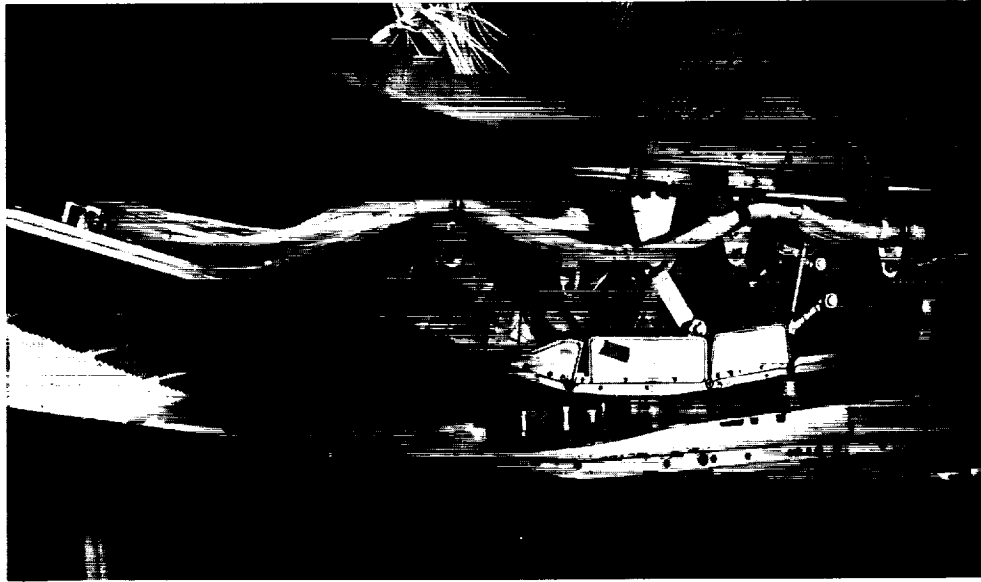
Inlet Model Installed in Wind Tunnel



CD-91-53930

A 1/3-scale model of the Mach 5 inlet was mounted on a trapezoidal plate in the NASA Lewis 10- by 10-Foot Supersonic Wind Tunnel. When set at a negative angle of attack, this plate accelerated the Mach 3.5 tunnel free-stream airflow to Mach 4.1, simulating airflow conditions on the first inlet ramp at Mach 5 cruise conditions. The accelerator plate was 100 in. wide, the inlet capture height (with the first ramp at 0° relative to free stream) and capture width were each 16 in., and the overall length of the model was approximately 20 ft. In addition to the variable ramp geometry, the model was equipped with remotely variable bleed exit plugs and main mass flow plug.

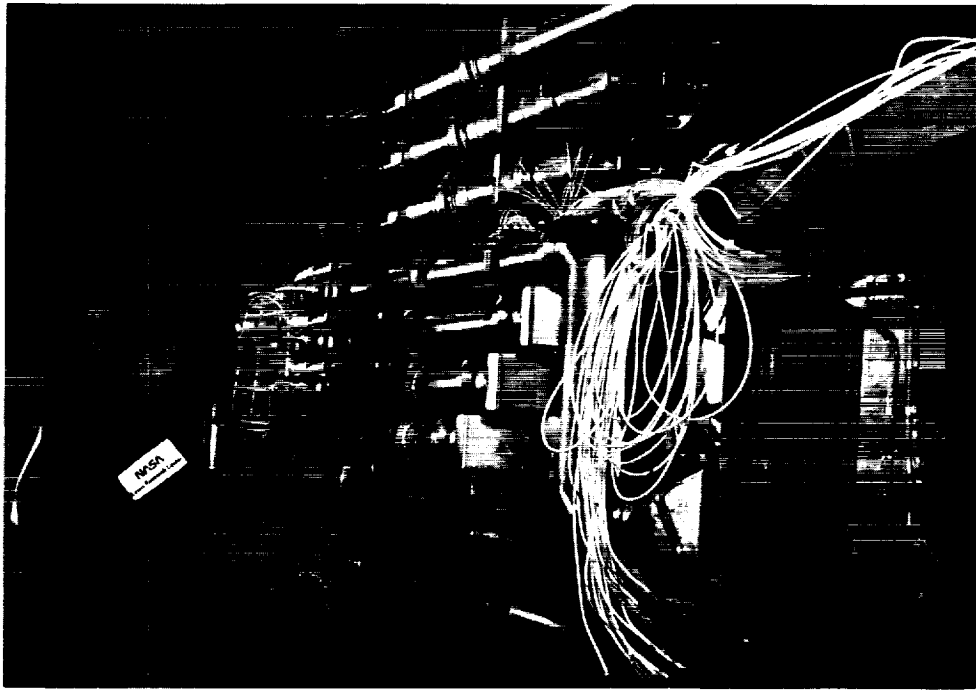
Inlet Model With Sidewall Removed



CD-91-53929

The near sidewall was removed from the inlet to reveal the linkages that control the movement of the variable ramp surfaces. Also visible are several of the model's porous bleed regions, each of which was compartmented and controlled by a separate exit plug. Since sidewall bleed regions extended beyond the ramp position at design conditions, as shown, the sealed plates perpendicular to the ramp surface near the wall prevented recirculation of bleed flow into the cavity above the ramp. Also visible is some of the model instrumentation, which included surface static taps, fixed total pressure rakes, translating pressure probes, and dynamic pressure transducers.

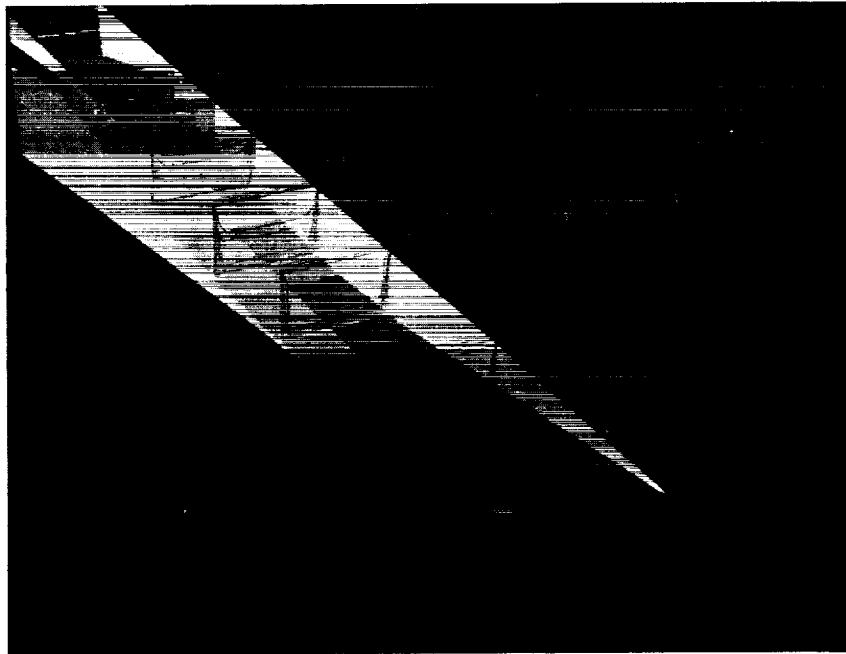
Inlet Sidewall Bleed Exit Plugs



CD-91-53928

The photograph shows remotely variable bleed exit mass flow plugs on the inlet sidewalls. Airflow through 15 bleed regions (5 on the ramp, 2 on the cowl, and 4 on each sidewall) was controlled and measured by conical exit plugs like these.

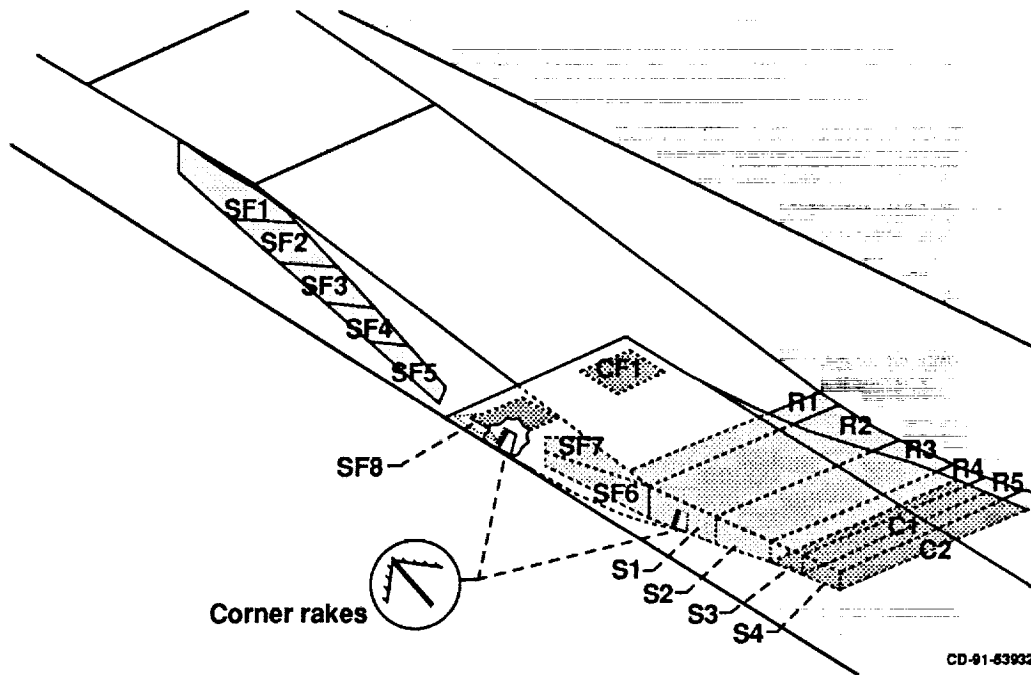
PNS Analysis of Mach 5 Inlet Mach Number Contours



CD-91-53831

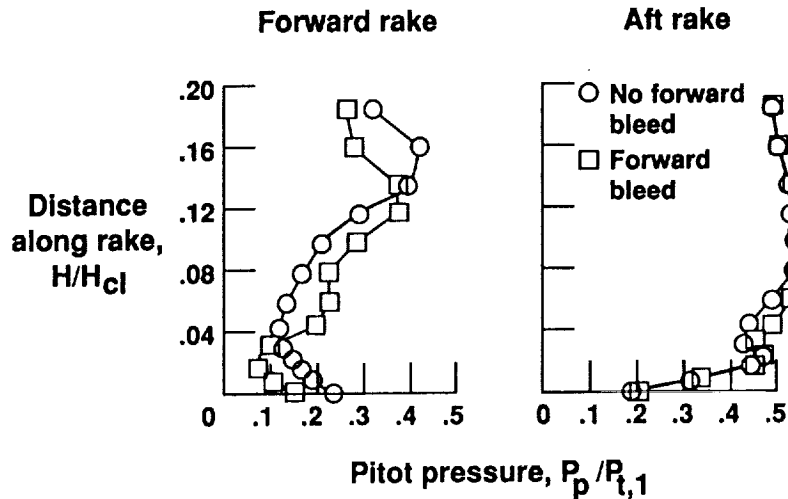
The Mach 5 inlet was designed two-dimensionally by using the method of characteristics, with the compression surfaces adjusted for displacement effects as predicted by viscous boundary layer codes. The first three-dimensional computational fluid dynamics (CFD) analysis was accomplished by Benson (ref. 2) using a parabolized Navier-Stokes (PNS) code, PEPSI-S (ref. 3). This analysis predicted a strong three-dimensional effect caused by the interaction of the ramp shock waves with the sidewall boundary layers. This glancing shock/boundary layer interaction phenomenon, which is described in more detail in reference 1, generated a vortical flow field near the sidewall boundary layer. This led, in turn, to boundary layer separations downstream of the cowl leading edge. This effect is illustrated in the figure, which shows Mach number contours at several inlet cross sections. The inlet, in this case, is inverted, with the cowl on the top. The farthest downstream cross section, aft of the cowl lip, indicates massive separations in the corner between the cowl and the sidewalls. Such separations, as indicated by this analysis, would likely lead to inlet unstart.

Inlet Bleed Regions and Corner Rake Locations



The figure indicates the locations of the various porous bleed regions on the inlet model. The original model design specified ramp bleed areas R1 to R5, cowl bleed areas C1 and C2, and sidewall bleed areas SF6 to SF8 and S1 to S4. Sidewall bleed regions SF1 to SF5 and cowl bleed region CF1 were added to the model design after the three-dimensional PNS analysis was completed. The purposes of this bleed were to diminish the three-dimensional flow phenomena caused by glancing shock/sidewall boundary layer interactions and to prevent separation on the cowl. Also shown are the locations of cowl corner rakes in the inlet. These rakes were oriented at an angle of 45° relative to the local cowl and sidewall surfaces. The farther upstream rake was located approximately 6 in. aft of the cowl leading edge (near the end of the first cowl corner bleed zone, $STA/H_{c1} = 3.73$), and the downstream rake was located 15 in. aft of the leading edge (slightly aft of the start of sidewall bleed region S1, $STA/H_{c1} = 4.28$). The placement of these rakes was chosen to coincide with the separation and vortical flow regions predicted by CFD.

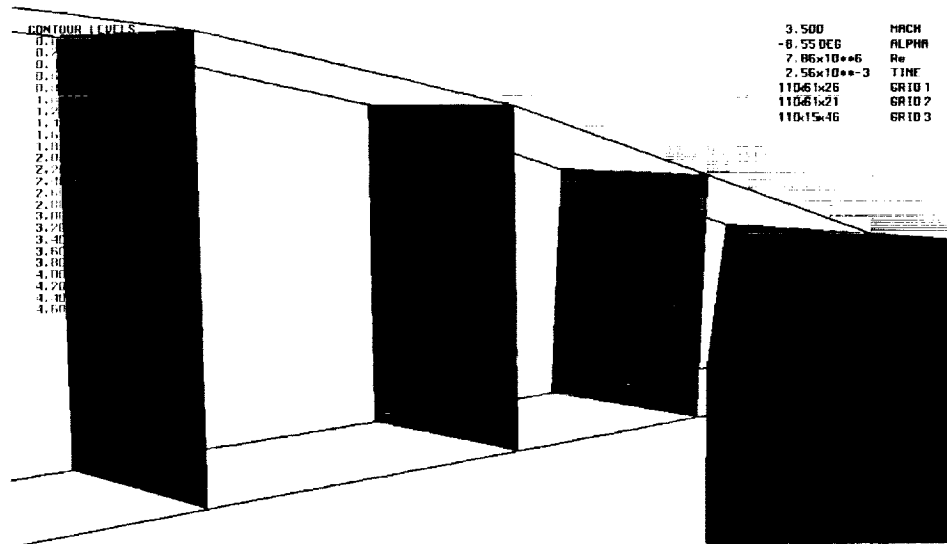
Cowl Corner Rake Pitot Pressure Profiles



CD-91-53933

Cowl corner rake pitot pressure profiles (nondimensionalized to tunnel total pressure $P_{t,0}$) are presented in the figure, data for the forward rake ($STA/H_{c1} = 3.73$) on the left and data for the aft rake ($STA/H_{c1} = 4.28$) on the right. For all data presented here the tunnel free-stream Mach number M_0 was 3.49, and the total pressure $P_{t,0}$ was 35.1 psia (this was also the total pressure on the first ramp $P_{t,1}$.) The angle of attack of the accelerator plate was -8.55° , providing a Mach number on the first ramp M_1 of 4.1, which simulated Mach 5 flight conditions. For all data presented here, bleed was removed from ramp bleed regions R1 to R5, cowl regions C1 and C2, and sidewall bleed regions S1 to S4. Bleed was also removed (square symbols) from sidewall bleed regions SF1 to SF8 and cowl corner bleed region CF1. These bleed regions were also closed off (circular symbols). The no-forward-bleed pitot pressure profile for the forward corner rake indicates large changes in pressure, with a region of medium pitot pressure near the corner that decreases rapidly, rises, and then decreases again near the end of the rake. The profile with forward bleed shows an additional small rise in pitot pressure after the initial falloff, and the pressure near the end of the rake fell off sooner. This seems to indicate that the rake was cutting across the zone of vortical flow in the cowl corner but that the flow was not the same with and without upstream bleed. Farther downstream (rake data shown on right), there is only a small "bump" in the profile near the corner, and bleed and no-bleed profiles are very similar. These data do not indicate the presence of vortical flow at this location. Either it has moved to an area where it cannot be detected by the rake, or it has been dissipated. In any case, upstream sidewall and cowl corner bleed seems to make little difference on the quality of the flow at this location.

Mach Number Contours Rose and Perkins



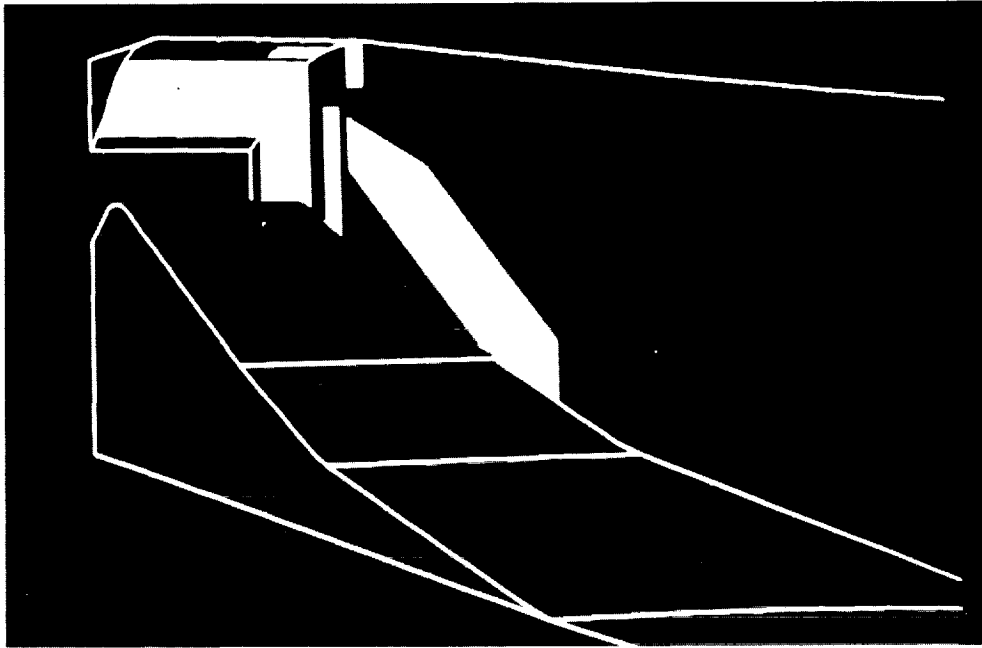
CD-91-53934

Several three-dimensional analyses of the inlet have been made recently using several codes. Two analyses are presented here, the first with a minimal amount of bleed (required to prevent the inlet from unstating), and the second with large amounts of bleed removed from many bleed regions, simulating an experimental bleed configuration.

The first analysis shows the nature of the vortical flow region described earlier and its behavior when no bleed is present to control it. Rose and Perkins (ref. 5) calculated the flow field in the Mach 5 inlet by using the SCRAM3D code. This code uses the Kumar explicit, time-accurate implementation of MacCormack's algorithm to solve the full Navier-Stokes equations (ref. 6). The figure shows Mach number contours for half of the inlet cross section at several axial stations, with the near side being the inlet sidewall. The ramp is at the top of the figure, and the plane that will contain the cowl is at the bottom. The first contour plane is located at the junction of compression ramps 1 and 2. The second contour is at the junction of ramps 2 and 3. The third contour is at some station along ramp 3, and the last contour is at the cowl lip station. The thickening of the sidewall boundary layer can be seen in the upstream planes. In the second and third planes, the thickest part of the layer moves down the sidewall and begins to show vortical behavior. The cowl lip can be seen in the fourth plane as the thin dark band across the bottom of the inlet. The contour at the cowl lip shows that about one-third of the vortical flow is spilled over the cowl lip.

Computational Bleed Zones

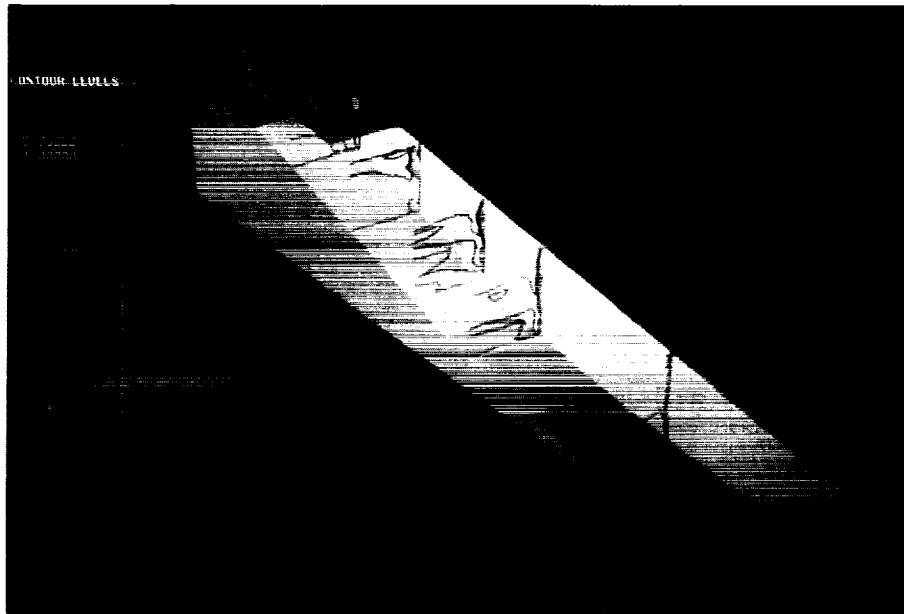
Reddy



CD-91-53935

Another calculation of flow through this inlet was accomplished by Reddy, Benson, and Weir (ref. 7). A time-marching code, PARC3D (ref. 8), which solves the full three-dimensional Reynolds-averaged Navier-Stokes equations in strong conservation form with the Beam and Warming approximate factorization, was selected for this calculation. The turbulence model used in the code was the Baldwin-Lomax model. The calculation included a simulation of the bleed through the zones indicated here. In this figure, and in subsequent figures showing CFD predictions, the inlet orientation has been inverted, with the cowl on the top. The bleed was simulated in the computations by imposing a constant mass flow (measured in the experiment) through the bleed surfaces. A previous calculation (ref. 9) with no bleed showed a separation bubble near the throat region that grew slowly with increasing iterations, indicating that the inlet would unstart. Some bleed was, in fact, required to keep the inlet model from unstating; thus, the calculation with bleed more accurately modeled the actual experimental conditions.

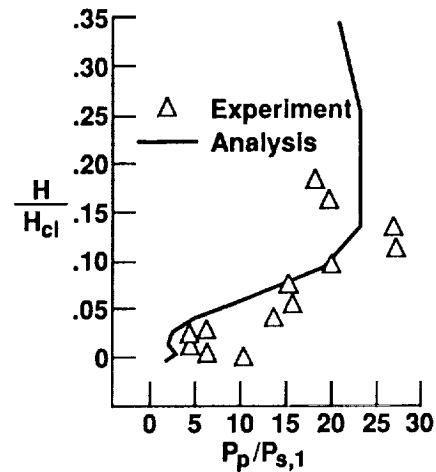
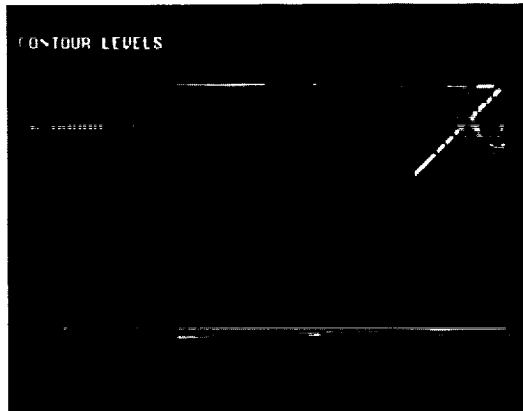
Mach Number Contours Reddy



CD-01-53936

The figure shows Mach number contours at several inlet cross sections. Only half of the inlet flow field has been computed, since the inlet is symmetric in the transverse direction. Strong secondary flow is visible; it is set up by shock/boundary layer interaction and by migration of low-energy flow up the sidewall and then toward the inlet centerline as it is captured by the cowl and heads toward the throat. As the flow approaches the throat bleed regions, it appears that most of the low-energy flow on the cowl and sidewalls has been removed and that the Mach number profiles are basically clean.

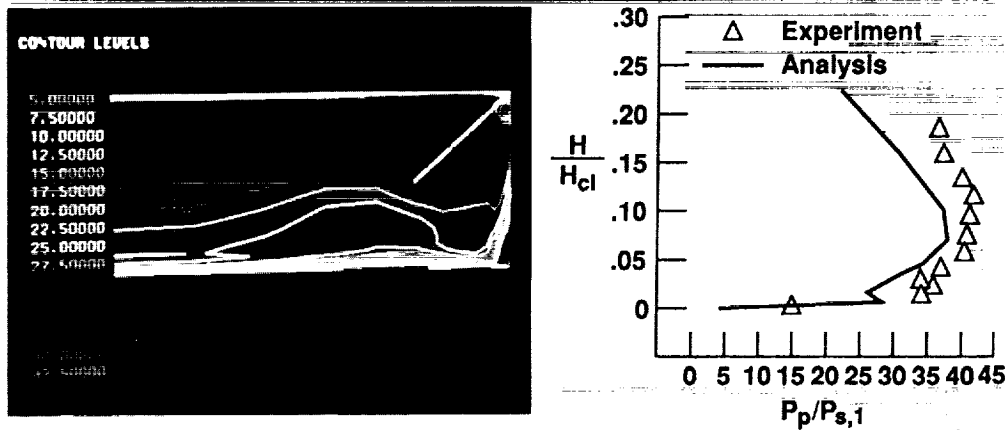
Comparison of Calculated and Experimental Upstream Corner Rake Data Reddy



CD-91-53937

On the left side of the figure the orientation of the rake at $STA/H_{cl} = 3.73$ is shown relative to the pitot pressure ratio contours at a nearby station. On the right the calculated rake pitot pressure (nondimensionalized to plate static pressure, $P_{s,1}$) profile (solid curve) is compared with the experimental data (triangular symbols) with bleed. Although the calculation does not agree extremely closely with the data, it does indicate large pressure fluctuations across the region of low-energy flow in the cowl corner, indicating the presence of the vortical flow.

Comparison of Calculated and Experimental Downstream Corner Rake Data Reddy



CD-91-53938

A figure similar to the previous one is shown for the downstream corner rake ($STA/H_{c1} = 4.28$). In this case the analysis somewhat underpredicts the value of the pitot pressure, but displays a similar shaped curve. The pitot pressure contours indicate that the low-energy corner flow has been mostly removed, leaving fairly uniform flow in the duct at that station. This is most likely due to the effect of bleed on the sidewalls through regions SF6, SF7, and S1 (refer back to the figure showing inlet bleed areas), which has apparently removed much of the low-energy flow.

CONCLUDING REMARKS

The research completed on the Mach 5 inlet at this time does not provide a complete understanding of the complex three-dimensional flow phenomena that are characteristic of rectangular inlets in this speed range. Further analysis and experimental data are required to determine the detailed flow physics that control the three-dimensional flow phenomena generated by shock/boundary layer interactions. However, some initial conclusions can be drawn from the data presently available. The analyses performed to date on the Mach 5 inlet agree that a vortical flow pattern is generated due to shock/boundary layer interactions. The data, particularly from the cowl corner rakes, tend to corroborate this. It is also generally agreed that bleed upstream on the sidewall, where the vortex is formed, has little effect on vortical flow. It appears that the nature of the vortical flow changes as it passes through the cowl shock and heads toward the throat, such that with bleed downstream the low-energy flow has been mostly removed and relatively uniform flow remains. Experimental data support this theory because the phenomena are no longer visible at the second corner rake station. Further analysis, data, or both are required to determine which bleed region or regions actually remove the low-energy flow.

In the future an identical test case (maximum bleed) will be run by using the SCRAM3D code to provide a direct comparison with the most recent PARC analysis. Other analytical efforts will involve modeling of alternative bleed configurations to determine the bleed locations required to remove the vortical flow. This effort will be supported by the second experiment phase, scheduled for August 1991. The primary objective of this phase will be to fully determine the performance of the inlet. However, additional data, including surface oil flow visualization, will be obtained where possible to help determine the size, extent, and behavior of the vortical flow.

REFERENCES

1. Perkins, E.W.; Rose, W.C.; and Horie, G.: Design of a Mach 5 Inlet System Model. NASA CR-3830, 1984.
2. Benson, T.J.: Three-Dimensional Viscous Calculation of Flow in a Mach 5.0 Hypersonic Inlet. AIAA Paper 86-1461, June 1986.
3. Anderson, B.H.: Three-Dimensional Viscous Design Methodology for Advanced Technology Aircraft Supersonic Inlet Systems. AIAA Paper 84-0194, Jan. 1984 (also NASA TM-83558).
4. Coltrin, R.E.: High-Speed Inlet Research Program and Supporting Analyses. Aeropulsion '87, NASA CP-3049, 1987, pp. 469-486.
5. Rose, W.C.; and Perkins, E.W.: Innovative Boundary Layer Control Methods in High Speed Inlet Systems. NASA CR-185206, 1990.
6. Kumar, A.: Numerical Simulation of Flow Through Scramjet Inlets Using a Three-Dimensional Navier-Stokes Code. AIAA Paper 85-1664, July 1985.
7. Reddy, D.R.; Benson, T.J.; and Weir, L.J.: Comparison of 3-D Viscous Flow Computations of Mach 5 Inlet With Experimental Data. AIAA Paper 90-0600, Jan. 1990 (also NASA TM-102518).
8. Cooper, G.K.; Jordan, J.L.; and Phares, W.J.: Analysis Tool for Application to Ground Testing of Highly Underexpanded Nozzles. AIAA Paper 87-2015, June 1987.
9. Weir, L.J.; Reddy, D.R.; and Rupp, G.D.: Mach 5 Inlet CFD and Experimental Results. AIAA Paper 89-2355, July 1989 (also NASA TM-102317).